J. Plasma Fusion Res. SERIES, Vol. 6 (2004) 719–722

Numerical Examination of Electromagnetic Field Properties in a Cylindrical Periodic Slow Wave Structure

YAMAZAKI Hoshiyuki, OGURA Kazuo and WATANABE Tsuguhiro[1]

Graduate School of Science and Technology, Niigata University, Niigata, 950-2181, Japan

[1]National Institute for Fusion Science, Toki, 509-5292, Japan

(Received: 9 December 2003 / Accepted: 26 February 2004)

Abstract

The previous studies of backward wave oscillators (BWOs) have been restricted in the operation at the fundamental axisymmetric TM mode. However, nonaxisymmetric operations of BWO are observed in the experiments and become important. In this work, the Rayleigh-Bessel (R-B) method is improved in order to analyze the nonaxisymmetric as well as axisymmetric fields in a periodic slow-wave structure (SWS). This method is based on the Rayleigh hypothesis, whose limit has been argued extensively. For the X-band SWS, the modulation depth is about 4 times of the theoretically established limit of the Rayleigh hypothesis. We compare the R-B method with another one based on a numerical integration of Maxwell equations, which is free from the Rayleigh hypothesis. The field properties derived by the R-B method show some singularities inside the corrugation due to the Rayleigh hypothesis. However, regardless the singularities, the dispersion characteristics and the fields outside the corrugation are in very good agreement with those by the numerical integration. The validity of the R-B method is discussed.

Keywords:

backward wave oscillator, X-band, periodic slow-wave structure, axisymmetric mode, nonaxisymmetric mode, Rayleigh hypothesis

1. Introduction

The slow-wave high-power microwave devices such as backward wave oscillator (BWO) have one element in common, that is a slow-wave structure (SWS) such as Fig. 1 [1]. It is very important and essential to know the field properties in the SWS, to understand and to use the wave-particle interaction in the slow-wave devices [1]. Theoretical and experimental studies have been performed extensively based on the axisymmetric transverse magnetic (TM) mode [2-5]. For the axisymmetric case, a pure transverse electric (TE) mode is ignored because it cannot interact with the beam in the slow-wave devices [6]. Recently, high-power BWO operations in nonaxisymmetric hybrid mode are demonstrated and become very important [6-8]. The previous studies of the slow-wave devices should be extended to nonaxisymmetric cases.

Periodic structures and gratings are widely used in modern science and technology such as optics, acoustic design, infrared spectroscopy and microwave technology [9,10]. Among the various methods to analyze such periodic systems, the Rayleigh methods are particularly simple and important [11-13]. They are based on the Rayleigh hypothesis that the fields inside the periodic corrugation are also expressed by the same spatial harmonic series as outside the corrugation. Its criterion of $2\pi h/z_0 < 0.448$ has been established theoretically with the Dirichlet boundary, based on a scattering of a plane wave by a sinusoidally corrugated surface, in a semi-infinite domain [10-12]. If this condition is not fulfilled ($2\pi h/z_0 > 0.448$), the spatial harmonic series expansion has singularities inside the corrugation. This means that the field expression using the harmonic series outside the corrugation is not continued analytically into the corrugation region. For the X-band SWS in Fig. 1, the modulation depth is about 4 times this limit. However, the experiment shows

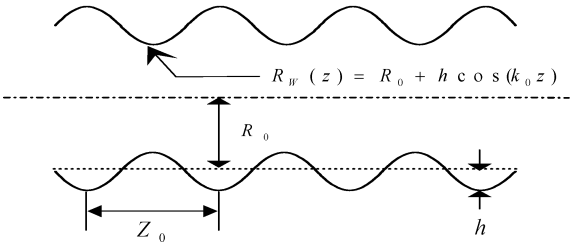

Fig. 1 X-band periodic SWS. The radius varies along the axial direction z as $R_0 + h\cos((2\pi/z_0)z)$ with R_0 = 14.45[mm], h = 4.45[mm], z_0 = 16.7[mm] and $2\pi h/z_0$ = 1.67.

Corresponding author's e-mail: f02j009g@mail.cc.niigata-u.ac.jp

excellent agreements with the Rayleigh-Bessel (R-B) method, one of the Rayleigh methods [2,3]. The agreement is shown not only by the dispersion characteristics but also by the field distributions of axisymmetric TM modes. The validity of the R-B method seems not to be determined by only the limit of the Rayleigh hypothesis, and should be examined more definitely. Moreover, for nonaxisymmetric cases, the normal mode becomes hybrid of TM and TE and the boundary condition should include both polarizations of TM and TE. The problems are mixed problems of Diricrhlet and Neumann boundaries.

This work is aimed at studying electromagnetic field properties of axisymmetric and nonaxisymmetric modes in the X-band SWS. We use two methods, one is the R-B method and the other is a numerical integration of Maxwell equations using the higher-order implicit difference method (HIDM) [14,15]. The latter is free from the Rayleigh hypothesis. The validity of the R-B method is discussed.

2. Numerical methods

In the R-B method, the temporal and spatial phase factor of all perturbed quantities is assumed to be $\exp[\mathrm{i}(k_z z + m\theta - \omega t)]$. Here, m is the azimuthal mode number and k_z is the axial wave number. Outside the corrugation ($r \leqq R_0 - h$), Floquet's theorem is exactly applicable. The axial electric and magnetic field components in the cylindrical system can be expresses as

$$E_z(z,r,t) = \sum_{p=-\infty}^{\infty} A_p J_m\left(\frac{k_p}{R_0} r\right) \exp\left[\mathrm{i}(k_p z + m\theta - \omega t)\right],$$

$$B_z(z,r,t) = \sum_{p=-\infty}^{\infty} B_p J_m\left(\frac{k_p}{R_0} r\right) \exp\left[\mathrm{i}(k_p z + m\theta - \omega t)\right], \quad (1)$$

where, J_m is the mth order Bessel function of the first kind, $k_p = k_z + pk_0$ and p is Floquet's harmonic number. The other field components are derived from eq. (1).

At the wall of SWS ($r = R_w$), two electric field components tangential to the wall, i.e. E_{lt} in the r-z plane and $E_{l\theta}$ in the θ direction, should be zero. A serious problem is how to express the electric field inside the corrugation. The Rayleigh hypothesis assumes that the fields inside the corrugation are also expressed by eq. (1). With this hypothesis, the spatial Fourier transform of the boundary conditions can be expressed as,

$$\begin{bmatrix} D^{(Z+)} & D^{(Z-)} \\ D^{(T+)} & D^{(T-)} \end{bmatrix} \cdot \begin{bmatrix} \boldsymbol{A} \\ \boldsymbol{B} \end{bmatrix} = 0 . \quad (2)$$

Here, $\boldsymbol{A}$ and $\boldsymbol{B}$ are column vectors with elements A_p and B_p, and $D^{(Z\pm)}$ and $D^{(T\pm)}$ are matrixes of an infinite rank. The dispersion relation is obtained from the condition that eq. (2) has a nontrivial solution and is given by

$$\det \begin{bmatrix} D^{(Z+)}(\omega, k_z) & D^{(Z-)}(\omega, k_z) \\ D^{(T+)}(\omega, k_z) & D^{(T-)}(\omega, k_z) \end{bmatrix} = 0 . \quad (3)$$

Equations (2) and (3) are a extended version of refs. [2-4] to nonaxisymmetric normal modes.

Another method free from the Rayleigh hypothesis is a numerical integration of Maxwell equations. Using the field expression of $\Phi(r, \theta, z) = r^m \varphi(r, z)\exp[\mathrm{i}(m\theta - \omega t)]$, the wave equations for TM and TE components can be expressed as the following form,

$$\varepsilon_0 \mu_0 \omega^2 \varphi + \frac{\partial^2 \varphi}{\partial z^2} + \frac{\partial^2 \varphi}{\partial r^2} + \frac{2m+1}{r} \frac{\partial \varphi}{\partial r} = 0 . \quad (4)$$

Without the expansion of eq. (1), the differential equations in the form of eq. (4) for TM and TE are numerically solved subjected to the given boundary conditions by using the computer code HIDEM [14,15]. Equation (4) is the elliptic differential equation and the solutions by the numerical integration are unique for appropriate boundary values.

3. Numerical analysis of field

Dispersion curves of the lowest axisymmetric and nonaxisymmetric normal modes are shown in Fig. 2. In the axisymmetric case (m = 0), $D^{(Z-)}$ and $D^{(T-)}$ become zero matrixes. Hence, eq. (3) gives pure TM_{0n} ($\det[D^{(Z+)}] = 0$) and TE_{0n} ($\det[D^{(T+)}] = 0$) modes. In the nonaxisymmetric cases, boundary conditions at the SWS wall combine TM and TE components. The normal modes become hybrid modes. Combinations of two letters, EH and HE, are commonly used for the designation of hybrid mode. Note that this definition is rather arbitrary. In this paper, the definition in the field of the plasma physics is used. In the limit of $h \to 0$, EH becomes TM and HE becomes TE. This is opposite to the definition based on the so-called normalized hybrid factor [9].

Fields patterns of TM_{01} and HE_{11} are shown in Figs. 3 and 4, respectively. Inside the corrugation, the patterns of two methods are quite different. For the R-B method, the singularities due to the Rayleigh hypothesis can be seen inside the corrugation for both TM_{01} and HE_{11}. These singularities move to the wall as decreasing the h, and disappear if the criterion of the Rayleigh hypothesis is fulfilled, $2\pi h/z_0 < 0.448$. The same behavior of the singularities is observed for pure TM and TE polarities, and also for the hybrid HE and EH modes. This means that the limit of the Rayleigh hypothesis independents of the TM/TE polarization and is applicable to the mixed problem of Diricrhlet and Neumann boundaries.

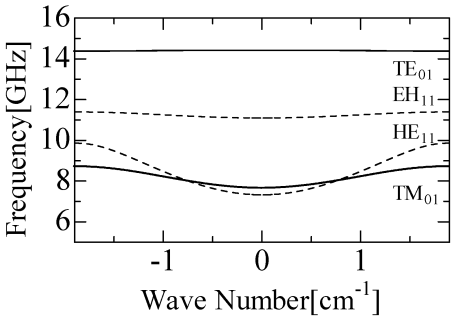

Fig. 2 Dispersion curves of TM_{01}, HE_{11}, HE_{11} and TE_{01}.

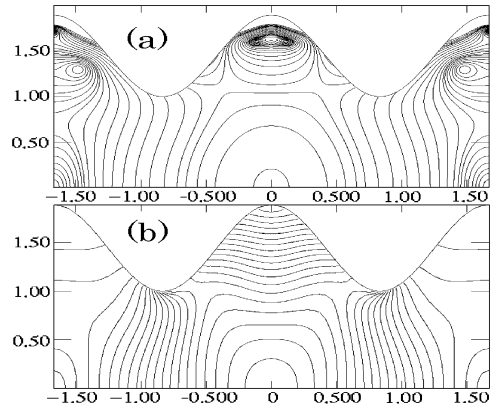

Fig. 3 Distribution of $|E|$ for TM_{01} at $k_z z_0 = 0.5\pi$, obtained by (a) the R-B method and (b) the integration method.

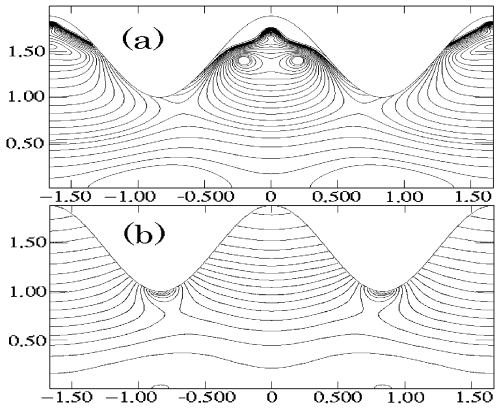

Fig. 4 Distribution of $|E|$ for HE_{11} at $k_z z_0 = 0.5\pi$, obtained by (a) the R-B method and (b) the integration method.

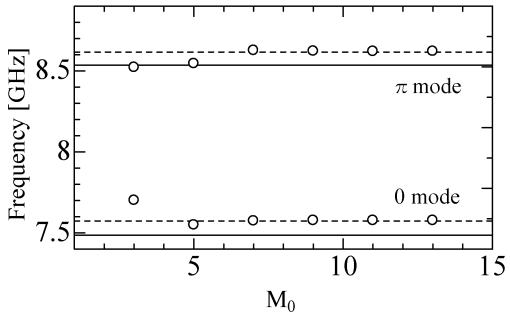

Fig. 5 The frequencies of the R-B method at $k_z z_0 = 0$ and π versus M_0. The frequencies of the numerical integration method (broken lines) and experiment (solid lines) are also shown.

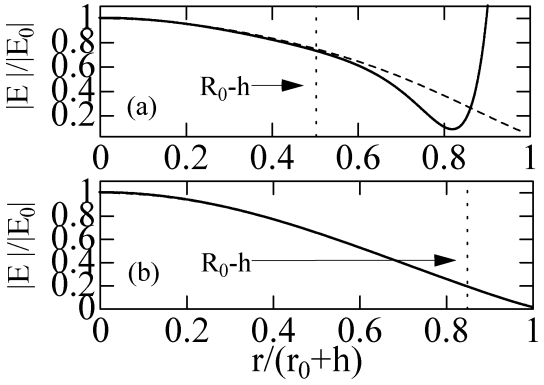

Fig. 6 Radial distribution of $|E|$ at $z = 0$ in Fig. 3 with (a) $2\pi h/z_0 = 1.67$ and (b) with $2\pi h/z_0 = 0.446$. The radial profiles of electric field by HIDM draws solid line, and that by R-B method draws broken line.

The singularities inside the corrugation do not disappear by increasing the matrix size M_0 of eqs. (2) and (3). This is because that the singularities are attributed to the Rayleigh hypothesis. For particular values of k_z, the field patterns of two methods differ near $r \approx R_0 - h$, at the top region of wall for pure TM and hybrid HE and EH, not TE, as shown in Fig. 4. The singularities affect the fields inside and near the corrugation. However, regardless the existence of singularity, the R-B method converges with increasing M_0, as can be seen in Fig. 5. Above $M_0 = 7$, the dispersion curves for axisymmetric and nonaxisymmetric modes are well converged. The convergent frequencies coincide excellently with those of the numerical integration, within 0.1 %.

In Fig. 6, radial profiles of electric field obtained by two methods are shown. They coincide in the entire region if the criterion of the Rayleigh hypothesis is fulfilled, $2\pi h/z_0 < 0.448$. For the X-band SWS, the field of the R-B method diverges near the wall due to the singularities and is slightly smaller than the numerical integration method in the region of $r \approx R_0$. However, the fields are almost the same outside the corrugation $r < R_0 - h$. The singularities may affect the coefficients of eq. (1) and change the fields inside and near the corrugation. This effect may appear as a change in effective R_0 and/or h, that is, sift of the dispersion curves. For the X-band SWS, the difference of two methods is very small and it can be said that the effect of singularity is effectively negligible outside the corrugation.

4. Discussion and summary

The R-B method can explain the experimental results. As an example, experimentally obtained dispersion characteristics are plotted in Fig. 7. They are in good agreement. The R-B method expects a slightly up-shifted curve, within 1 %. Manufacture accuracy of the SWS is of the order of 0.1 mm and can lead this difference. For example, the numerical dispersion characteristics almost completely coincide with the experimental results if R_0 and h increased by 0.14 mm (1 %) and 0.04 mm (1 %), respectively. Detailed comparison of the R-B method and experiment have been reported in Refs. [2-4]. In these experiments, not only the dispersion characteristics but also the field profiles outside the corrugation are examined experimentally and are well fitted by the R-B method.

The validity of the R-B method can be argued from two criteria.

(a) No singularities inside the corrugation ($r > R_0 - h$).

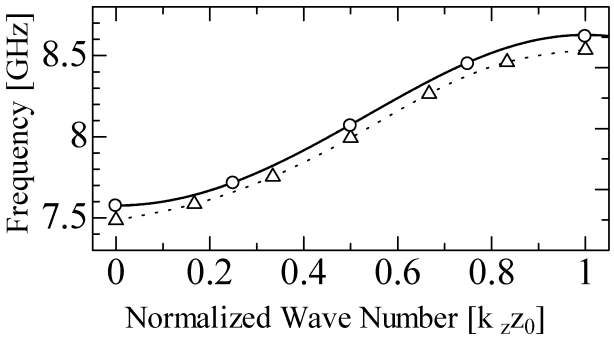

Fig. 7 Comparison of dispersion characteristics: the R-B method with M_0 = 7 (solid line), the numerical integration method (circle) and the experiment data (triangle).

(b) The convergence outside the corrugation ($r < R_0 - h$).

The criterion (a) is the limit of the Rayleigh hypothesis. In this work, this limit is clearly shown by the appearance and disappearance of the singularities in the physical mapping. The criterion of $2\pi h/z_0 \approx 0.448$ is confirmed for TM and TE polarization by changing h. However, the failure of (a) does not mean directly the unavailability of the R-B method as is presented and discussed in this paper. The field expression of eq. (1) is strictly valid outside the corrugation. The convergent solution of the R-B method is very close to the field obtained by the numerical integration by HIDM. It can be concluded that the expansions in the R-B method converge closely to the unique solution of the X-band SWS, independently of whether the Rayleigh hypothesis is satisfied or not. This may be the reason why the R-B method is in good agreement with the X-band experiment in Fig. 7 and Refs. [2-4]. The existence of singularities may affect the coefficients. The detailed and systematic study on this effect is required in order to obtain the more general criterion for the Rayleigh methods.

Acknowledgements

This work was partially supported by a Grant-in-Aid for Scientific Research from the Ministry of Education, Science, Sports and Culture of Japan. Support of numerical calculations was afforded by the Computer Center, National Institute for Fusion Science.

References

[1] J. Benford and J. Swegle, *High-Power Microwaves* (Artech House, Norwood, MA, 1992).
[2] W. Main *et al.*, IEEE Trans. Plasma Sci. **22**, 566 (1994).
[3] Md.R. Amin *et al.*, IEEE Trans. Microwave Theory Tech. **43**, 815 (1995).
[4] Md.R. Amin *et al.*, J. Phys. Soc. Jpn. **65**, 627 (1996).
[5] S. Kobayashi *et al.*, IEEE Trans. Microwave Theory Tech. **26**, 947 (1998).
[6] K. Ogura *et al.*, Jpn. J. Appl. Phys. **42**, 7095 (2003).
[7] D.M. Goebel *et al.*, IEEE Trans. Plasma Sci. **26**, 354 (1998).
[8] S. Banna *et al.*, IEEE Trans. Plasma Sci. **28**, 798 (2000).
[9] P.J.C. Clarricoats and A.D. Olver, *Corrugated Horns for Microwave Antennas* (Peter Peregrinus, London, 1984).
[10] E.C. Loewen and E. Popov, *Diffraction Gratings and Application* (Marcel Dekker, Inc., NewYork, 1997).
[11] R.F. Millar, Proc. Cambridge Philos. Soc. **65**, 773 (1969) and **69**, 217 (1971).
[12] R.F. Millar, Radio Sci. **8**, 785 (1973).
[13] L. Kazandjian, Phys. Rev. E **54**, 6802 (1996).
[14] T. Watanabe *et al.*, J. Phys. Soc. Jpn. **61**, 1136 (1992).
[15] T. Watanabe *et al.*, Nucl. Instrum. Methods A **331**, 134 (1993).